JOC Article
pubs.acs.org/joc

DFT Study of Cycloparaphenylenes and Heteroatom-Substituted Nanohoops

Steven M. Bachrach* and David Stück†

Department of Chemistry, Trinity University, 1 Trinity Place, San Antonio, Texas 78212.
†Current address: Department of Chemistry, University of California−Berkeley, Berkeley, California 94720

sbachrach@trinity.edu

Received July 12, 2010

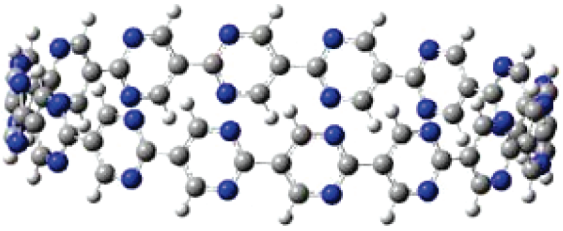

Nanohoops are macrocycles formed of aromatic rings linked in a 1,4′ fashion. Cycloparaphenylenes **1** and nitrogen analogues formed from the building blocks pyridinyl (**2**), pyrazinyl (**3**), pyridazinyl (**4**), and pyrimidinyl (**5**) are examined at B3LYP/6-31G(d). The nanohoops contain 3−24 repeat units. The strain energy of the nanohoops exponentially decreases with the number of building blocks *n*, and this strain strongly correlates with the bend angle at the *ipso* carbons. Nitrogen substitution reduces the *o*,*o*′ steric interactions between neighboring rings. Nanohoops **3** and **5** have ribbon-like structure with dihedral angles between neighboring rings near zero. Nanohoops **5** are the least strained and, with their ribbon structure, are suggested as synthetic targets for possible interesting bulk properties and structures.

1. Introduction

Among the ever-growing family of interesting organic nanostructures are the "nanohoops", cycloparaphenylenes **1** being the first examples of this class. These nanohoops are of recent interest as segments of armchair nanotubes.[1] From a more fundamental viewpoint, in closing paraphenylenes into a ring, a strain is produced, typically by an angle distortion at the *ipso* carbon atoms. This strain might be taken at the expense of aromaticity of the individual phenyl rings. Though these structures are obvious extensions of benzene and biphenyl, the cycloparaphenylenes were only recently synthesized. Bertozzi[2] prepared the [9]-, [12]-, and [18]-cycloparaphenylenes in 2008, and subsequently an alternative synthesis of [12]-cycloparaphenylene was reported[3] along with the preparation of [8]-cycloparaphenylene.[4]

As we were concluding our studies,[5] Itami and coworkers[6] reported the computed structures and strain energies of the [6]- through [20]-cycloparaphenylenes. They optimized structures at B3LYP/6-31G(d) and performed a thorough conformational landscape search for [12]-cycloparaphenylene and the smaller rings. For all cases, the lowest energy conformer had the phenyl rings canted alternately in opposite directions. The larger nanohoops were then optimized with this alternating ring geometry. Their other major finding was the exponential decrease of the strain energy with the size of the macrocycle. Nonetheless, the largest analogue, [20]- cycloparaphenylene, possesses a significant strain energy of 28.4 kcal mol^{-1}.

This alternating canted arrangement of the phenyl groups (see Figure 1) arises from *o*,*o*′ interactions as found in biphenyl. The cycloparaphenylenes thus do not possess a ribbon-like structure, which one might associate with an idealized hoop. In order to produce a ribbon, one must

(1) Dai, H. *Acc. Chem. Res.* **2002**, *35*, 1035–1044.
(2) Jasti, R.; Bhattacharjee, J.; Neaton, J. B.; Bertozzi, C. R. *J. Am. Chem. Soc.* **2008**, *130*, 17646–17647.
(3) Takaba, H.; Omachi, H.; Yamamoto, Y.; Bouffard, J.; Itami, K. *Angew. Chem., Int. Ed.* **2009**, *48*, 6112–6116.
(4) Yamago, S.; Watanabe, Y.; Iwamoto, T. *Angew. Chem., Int. Ed.* **2010**, *49*, 757–759.
(5) Stuck, D.; Bachrach, S. M. In *239th ACS National Meeting*; San Francisco, CA, 2010.
(6) Segawa, Y.; Omachi, H.; Itami, K. *Org. Lett.* **2010**, *12*, 2262–2265.

DOI: 10.1021/jo101371m Published on Web 09/09/2010

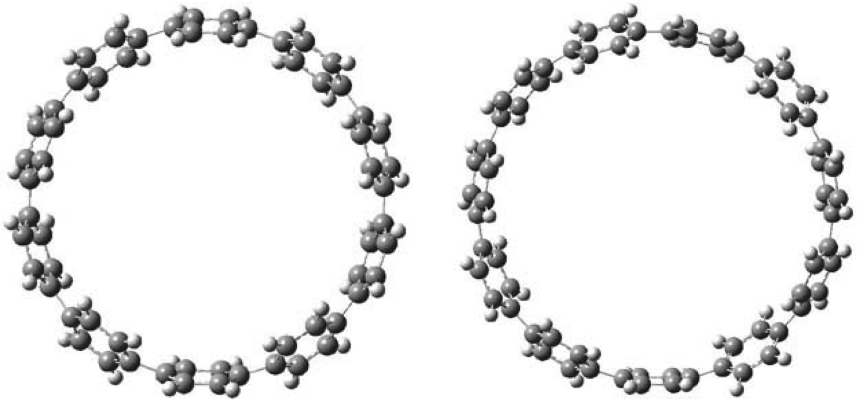

FIGURE 1. B3LYP-optimized geometries of [10]-**1** and [11]-**1**.

remove these interactions. We supposed that replacing the *ortho* carbon with a nitrogen atom would eliminate the *o*,*o*′ steric interaction. A reinforcement of the ribbon might also be affected through a weak stabilizing interaction between the nitrogen lone pair and the *o*′-hydrogen. We therefore extend the nanohoops to the cycloparapyridinylenes **2**, cycloparapyrazinylenes **3**, cycloparapyridazinylenes **4**, and cycloparapyrimidinylenes **5**. In particular we will employ density functional theory to evaluate their structures and their strain energies.

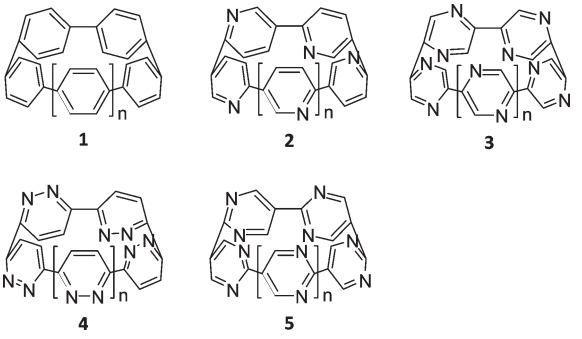

2. Computational Methods

The conformational space of the cycloparaphenylenes can be quite extensive as one considers whether successive rings are canted in opposite directions (as in the C_{2h} triphenylene **6a**) or in the same direction (helical as in the D_2 triphenylene **6b**). Itami has shown that the alternating back and forth ring arrangements (like **6a**) are preferred in the [6]- through [12]-phenylenes.[6] We assume this same conformational preference for the nanohoops **2**−**5**. Nanohoops **2**, **3**, and **4** have an additional conformational feature: whether the nitrogens on successive rings are on the same face of the ribbon or on opposite faces. We tested for a preference in this orientation for some of the small analogues of these three macrocycles. Otherwise, every structure was completely optimized within appropriate point groups at B3LYP/6-31G(d).[7] Each structure was confirmed to be a local energy minimum by analytical frequency analysis. Electronic energies were corrected for zero-point vibrational energy. In addition, the family of paracyclophanes **1** was fully optimized (and confirmed as local minima with vibrational frequency analysis) at MO6-2x/6-31G(d).[8−10] All computations were performed using Gaussian-09.[11]

Nanohoops **1**−**5** were studied with $n = 3-16$. The larger even-numbered hoops were also examined through $n = 24$. Compounds are designated as [*n*]-**X**, where *n* indicates the number of constituent rings and **X** indicates nanohoops of type **1**−**5**.

3. Results and Discussion

3.1. Benchmarking the Computational Method. The strain energy of the nanohoops, and the implications of this strain, is the main focus of this paper. Therefore, we will benchmark our computations though examination of the strain energy of the paracyclophenylenes **1**. Itami and co-workers[6] employed the B3LYP/6-31G(d) method, a workhorse among computational organic chemists for many years, though it has recently been shown to fail in some very basic ways, like ordering the constitutional isomers of alkanes.[12,13] This failure often becomes more acute with increasing size of the molecules. Nonetheless, because of its widespread use, we were inclined to also use the B3LYP functional if it could produce reasonable values of the strain energies for **1**. We therefore optimized the structures of **1** for $n = 3-16$, 18, and 20 at both B3LYP/6-31G(d) and M06-2x/6-31G(d).[8−10] This latter functional was developed particularly to address the failings of B3LYP[12−16] and has been demonstrated to provide excellent energies of, among other things, alkane isomers.[9,17]

(7) Becke, A. D. *J. Chem. Phys.* **1993**, *98*, 5648–5650.
(8) Zhao, Y.; Truhlar, D. G. *Theor. Chem. Acc.* **2008**, *120*, 215–241.
(9) Zhao, Y.; Truhlar, D. G. *Acc. Chem. Res.* **2008**, *41*, 157–167.
(10) Zhao, Y.; Truhlar, D. G. *J. Phys. Chem. A* **2008**, *112*, 1095–1099.
(11) Frisch, M. J.; et al. et al. *Gaussian-09*; Gaussian, Inc.: Wallingford, CT, 2009.
(12) Schreiner, P. R.; Fokin, A. A.; Pascal, R. A.; deMeijere, A. *Org. Lett.* **2006**, *8*, 3635–3638.
(13) Wodrich, M. D.; Corminboeuf, C.; Schleyer, P. v. R. *Org. Lett.* **2006**, *8*, 3631–3634.
(14) Check, C. E.; Gilbert, T. M. *J. Org. Chem.* **2005**, *70*, 9828–9834.
(15) Grimme, S.; Steinmetz, M.; Korth, M. *J. Org. Chem.* **2007**, *72*, 2118–2126.
(16) Pieniazek, S. N.; Clemente, F. R.; Houk, K. N. *Angew. Chem., Int. Ed.* **2008**, *47*, 7746–7749.
(17) Zhao, Y.; Truhlar, D. G. *Org. Lett.* **2006**, *8*, 5753–5755.

TABLE 1. Strain Energy (SE, kcal mol^{-1}) of 1 Using Reaction 1

n	B3LYP	MO6-2x
3	190.02	189.70
4	144.01	144.38
5	117.14	118.70
6	97.18	98.35
7	85.08	86.63
8	73.32	73.54
9	66.74	68.54
10	58.89	59.27
11	54.74	56.37
12	49.03	50.23
13	46.31	48.08
14	41.95	44.07
15	40.08	42.36
16	36.60	35.38
18	32.40	35.75
20	29.00	32.64
22	26.62	
24	24.07	

We use reaction 1 as a measure of the strain energy (SE) of **1**. This is a group equivalent reaction[18] that conserves not only the Benson group equivalents but also the number of phenyl rings with *para* substitution. Reaction 1 was also used by Itami,[6] though we report the strain energy at 0 K. The strain energy of each cycloparaphenylene is listed in Table 1, computed at both B3LYP and M06-2x. Our B3LYP/6-31G(d) results are consistent with Itami's results.

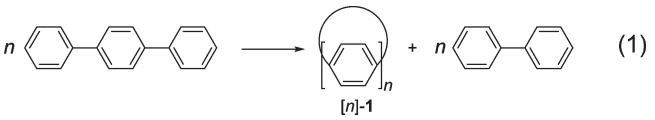

(1)

Inspection of Table 1 readily reveals that the two methods provide very close estimates of strain energies. The mean unsigned error between the two methods is 1.5 kcal mol^{-1}, and the maximum difference is 3.6 kcal mol^{-1} for the very largest system, [20]-**1**. The plot of strain energies computed by the two methods gives a linear fit, with a correlation coefficient of 0.9994 (see Figure S1). Furthermore, both methods predict that the alternating phenyl ring conformer (as in **6a**) is the lowest energy conformation, and the relative energy ordering of the other conformers is generally in close agreement. The dihedral angles between adjacent phenyl groups ($C_o-C_{ipso}-C_{ipso'}-C_{o'}$) are quite similar for the B3LYP and MO6-2x structures, differing by an average of 1.6°, with the M06-2x values always larger than the B3LYP values. This reflects in part the fact that M06-2x predicts a dihedral angle of 38.67° in triphenylene, while B3LYP predicts a smaller value of 37.40°. Overall, there is fine agreement between the two methods, and so we will report B3LYP values from here on.

3.2. Structures and Strain Energies of [*n*]-1. The lowest energy structures of the even cycloparaphenylenes generally are of $D_{(n/2)h}$ symmetry, while the odd members are of C_2 symmetry. These point groups require the phenyl rings to be canted in alternating opposite orientations, as in the D_2 triphenylene **6a**. An example of this is shown in Figure 1 for [10]-**1**. However, the odd members of **1** must have one phenyl group whose neighbors are arranged in the helical form of **6b**. An example of the odd members is [11]-**1**, also shown in Figure 1. The local helical arrangement of the phenyl rings

(18) Bachrach, S. M. *J. Chem. Educ.* **1990**, *67*, 907–908.

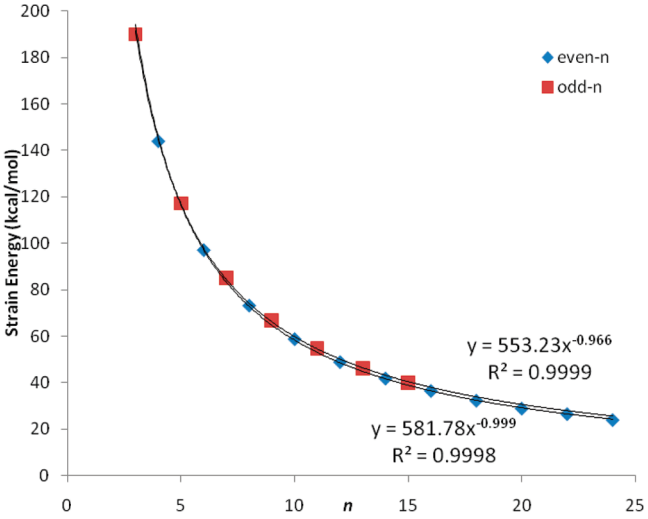

FIGURE 2. Correlation between *n* and strain energy for [*n*]-**1**.

appears at the bottom of this figure. The dihedral values (see Table S1) of the even members systematically increase with *n*, ranging from 18.5° in [4]-**1** to 35.3° in [24]-**1**, which is just shy of the value in **6a** (37.4°). The trend is similar among the odd members, but because of lower symmetry and the one helical arrangement, the dihedral angles span a range within each member. The value of the dihedral angle associated with the helical twist increases with *n*, from 8.2° in [5]-**1** to 26.8° in [15]-**1**.

In order to close a polyphenylene chain into a loop, the $C_{1'}-C_1-C_4$ angle must be contracted from linearity. This bend angle smoothly increases from the smallest loop, [3]-**1**, where its value is a very contracted 120.0°, to a value of 172.3° in the largest loop, [24]-**1**. Even in this large ring, the *ipso* carbons must distort more than 7° from its ideal (linear) value. The list of values of the bend angles for all cycloparaphenylenes is given in Table S1.

Itami[6] published a plot of *n* versus the strain energy of **1** and noted an inverse proportionality with the strain energy approaching zero kcal mol^{-1} as *n* approaches infinity. Close inspection of this curve (Figure S2) reveals that although all strain energies can be fit to a power function (SE = $578.75n^{-0.993}$) with a correlation coefficient of 0.9993, there are in fact two curves (see Figure 2), one for the even members (with $R = 0.9998$) and one for the odd members (with $R = 0.9999$) of the series. The two different curves result from their inherent differences in the dihedral angles between adjacent rings. The even members have exclusively alternating rings (as in **6a**), which is the energetically most favorable arrangement. The odd members must have one helical arrangement (as in **6b**), and this leads to the odd members being slightly more strained than the even congeners.

Implied by Figure 2 is that the strain energy per phenyl group decreases with increasing *n*. The intermediate sized nanohoop [12]-**1** has a strain energy per phenyl group of 4 kcal mol^{-1}. It is only with the largest nanohoops, i.e., [24]-**1**, that the strain energy per phenyl ring is only 1 kcal mol^{-1}, but this still means a total SE of 24 kcal mol^{-1}.

One might imagine that though a dihedral value less than that in **6a** would add strain to the molecules, the dominant contributor to strain in **1** is that due to distorting the $C_{1'}-C_1-C_4$ angle away from linearity. This distortion is what

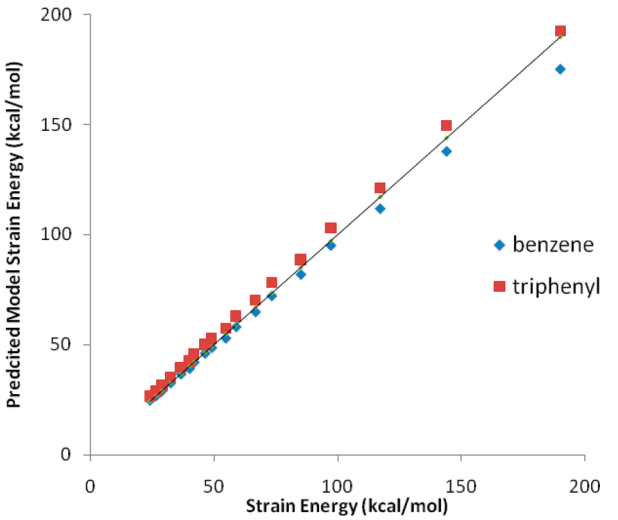

FIGURE 3. Correlation of the predicted strain energy from the benzene (**7a**) and triphenyl (**7b**) bending models and the strain energy for [*n*]-**1** computed with reaction 1. The drawn line represents the relationship with a slope of unity.

SCHEME 1. Definition of Bend Angle

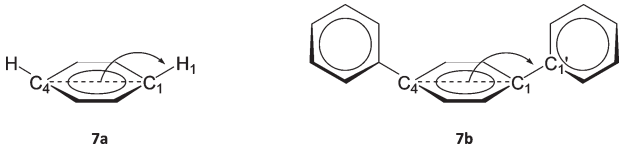

7a **7b**

allows the chain to wrap around and close into a loop. We assess the strain due to this bending at the *ipso* carbons in two ways: (a) comparing the energies of benzene with that of a C_{2v}-distorted benzene where the *para* hydrogens are raised out of the plane by an angle equivalent to that in the cycloparaphenylene series (**7a**) and (b) comparing the energies of triphenyl with that of a C_s-distorted triphenyl molecule where the terminal phenyl rings are bent out of plane (**7b**). The values of the model strain energies computed at B3LYP/6-31G(d) are listed in Table S2.

The model strain energy is the strain in a single phenyl ring due to the two distortions at the *para* carbons. Multiplying this energy by the number of rings in the nanohoop gives an estimate of the *total* strain energy in the nanhoop. Figure 3 displays a plot of the predicted total strain energy using both the benzene and triphenyl models and the computed strain energy from reaction 1. Both models provide fine estimates of the true strain energy, with excellent linear correlations. The benzene model slightly understimates the SE, due most likely to lack of inclusion of the *o,o′* steric interactions. The triphenyl model slightly overestimates the SE. Nonetheless, the SE of the cycloparaphenylenes is largely accounted for by the energy necessary to distort the *ipso* carbon atoms so as to close the loop.

Another potential strain within the cycloparaphenylenes occurs at the *ortho* carbons, where the bonded atoms are not all coplanar. The distortions from planarity are to minimize *o,o′* interactions and help accommodate the severe angle bend at the *ipso* carbon. The degree of nonplanarity can be assessed as the deviation of the sum of the three angles about the *ortho* carbon from 360°. For the most strained

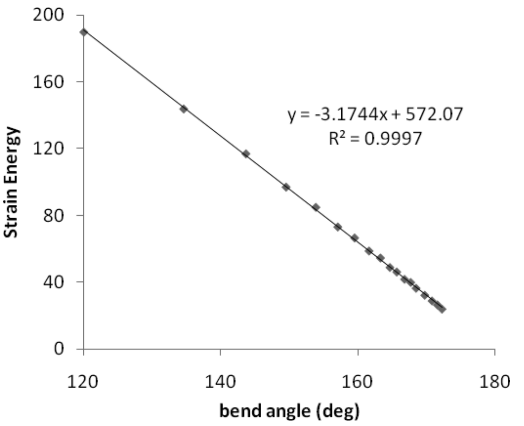

FIGURE 4. Correlation between the bend angle (C_i–C_1–C_4) and strain energy (kcal mol^{-1}) of **1**.

cycloparaphenylenes, this deviation is rather small: 2.5° in [3]-**1**, 1.9° in [4]-**1**, 1.4° in [5]-**1**, and 1.1° in [6]-**1**. One can estimate the energetic consequence of this strain by optimizing benzene with the three angles about each *ortho* carbon fixed to that found in the cycloparaphenylene and comparing this energy with that of D_{6h} benzene. With the angles fixed to that in [3]-**1** and [4]-**1**, the *ortho* strain energy per phenyl ring is 7.0 kcal mol^{-1} for [3]-**1** and 4.4 kcal mol^{-1} for [4]-**1**. This accounts for less than 1/7 of the total strain energy for these nanohoops. Furthermore, this *ortho* distortion is largely an accompaniment to the *ipso* strain. The angle sum at the *ortho* carbons of the model benzene distorted at the *ipso* carbon (as described above) nearly totally matches that in the cyclophane itself. Therefore, the *ipso* carbon strain model captures the strain energies at both the *ipso* and *ortho* carbons.

One can simplify this argument further. The degree of bending distortion in benzene can be related to the increase in its strain energy through a power series (see Figure S3). This suggests that the strain energy of each member of **1** is related to its bend angle, and this relationship is in fact linear, as demonstrated in Figure 4. This relationship predicts that a nanohoop of infinite size ([∞]-**1**), which would have a bend angle of 180°, would have a strain energy of 0.68 kcal mol^{-1}, in excellent agreement with the expected nil SE. Therefore, the simple measure of the bend angle in a nanohoop should be an excellent predictor of its overall strain energy.

3.3. Structures and Strain Energies of [*n*]-2, [*n*]-3, [*n*]-4, and [*n*]-5. The twisting in biphenyl and triphenyl is due to steric interaction between the *ortho* hydrogen atoms and is responsible for the alternating canted ring structure of **1**. Replacement of an *ortho* carbon and its attached hydrogen with a nitrogen atom might reduce this steric interaction and lead to a more ribbon-like nanohoop. We optimized the structures of four nitrogen analogues of biphenyls **8**–**11**. All four do have smaller dihedral angles between the rings than in biphenyl (where the dihedral angle is 37.4°), and in fact **9**, **10**, and **11** are planar (Figure 5). For these three, removal of two *o,o′* steric interactions is sufficient to allow for the conjugation between the two rings to dictate a planar arrangement.[19] In addition, a weak electrostatic interaction between the nitrogen lone pair and the *ortho* hydrogen is likely to be stabilizing the planar arrangement. This planarity suggests

(19) Bachrach, S. M. *J. Phys. Chem. A* **2008**, *112*, 7750–7754.

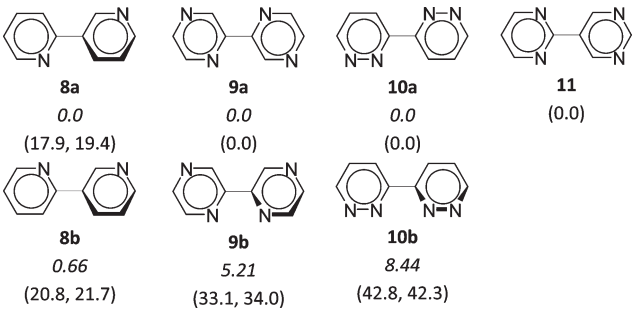

FIGURE 5. Relative energies (in italics) and dihedral angles between the rings for the lowest energy conformers of **8**−**11**.

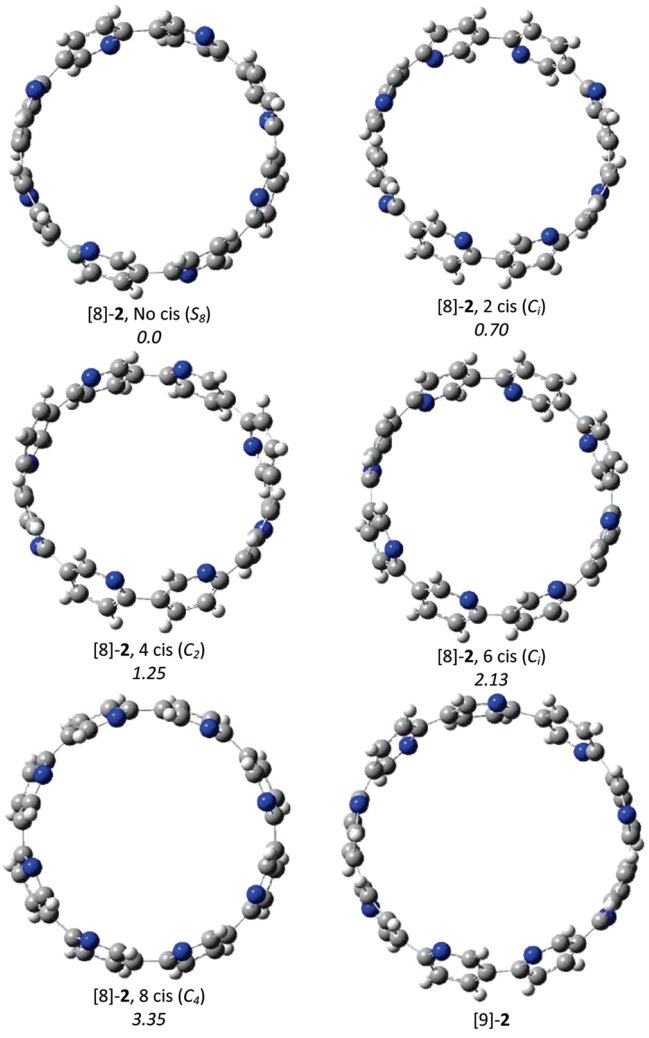

FIGURE 6. Conformers of [8]-**2** (with their number of *s-cis* arrangements, point groups, and relative energies (in kcal mol^{-1}) and the lowest energy conformer of [9]-**2**.

that nanohoops constructed of these nitrogen analogues might produce a ribbon structure.

Nitrogen substitution introduces another conformational complexity: whether the nitrogens are arranged *s-cis* or *s-trans*, as seen in **8a** versus **8b**, **9a** versus **9b**, and **10a** versus **10b**. The conformations of **8** have been computed previously

(20) Lehtonen, O.; Ikkala, O.; Pietilä, L.-O. *J. Mol. Struct.* (*THEOCHEM*) **2003**, *663*, 91–100.

TABLE 2. Strain Energy (SE, kcal mol^{-1}) of 2−5 using Reactions 2−5

n	2	3	4	5
3		150.45	175.64	
4	126.61	112.65	128.24	115.47
5	101.62	89.95	108.65	92.73
6	84.35	74.91	85.17	77.08
7	72.53	64.19	80.14	65.78
8	63.04	56.13	63.61	57.23
9	56.30	49.86	64.21	50.56
10	50.27	44.82	50.72	45.18
11	45.88	40.70	53.84	40.66
12	41.64	37.22	41.99	36.86
13	38.59	34.25	46.49	33.65
14	35.31	31.75	35.60	30.81
15	33.17	29.46	41.01	28.35
16	30.62	27.52	30.71	26.19
18	26.89	24.21	26.90	22.47
20	23.84	21.51	23.82	19.30
22	21.34	19.26	21.25	16.74
24	19.19	17.29	19.00	14.37

with a variety of methods,[20,21] and the *s*-trans conformer is preferred by a fraction of a kcal mol^{-1}, consistent with our computations. This preference is understood as minimizing the interaction of the dipole moments associated with each pyridinyl ring. HF/STO-3G computations of **9** and **10** find the planar *s-trans* conformer to be the preferred conformation, with a second minimum associated with an *s-cis* but nonplanar arrangement,[22] and we find the same result with B3LYP/6-31G(d). These *s-cis* conformers are destabilized by the very unfavorable interaction of the nitrogen lone pairs on the adjacent rings. These lone pair repulsions lead to a large energy difference in the conformations: **9a** is 5.2 kcal mol^{-1} lower in energy than **9b**, and the difference is even larger, 8.4 kcal mol^{-1}, between **10a** and **10b**.

It is therefore reasonable to expect that the nanohoops built from these nitrogen-substituted components will prefer to have the nitrogen atoms on opposite faces of the hoops. To confirm this expectation, we optimized a number of conformations of the smaller nanohoops **2**−**4**, varying the number of *s-cis* N−N interactions. A representative example is the conformational space of [8]-**2**; the conformers' structures and relative energies are shown in Figure 6. (Comparable structures of [8]-**3** and [8]-**4** are shown in Figures S3 and S4.) The S_8 conformation of [8]-**2** has no *s-cis* arrangements and is the lowest energy conformer. The next lowest energy conformer has two *s-cis* arrangements (these must come in pairs for the even nanohoops), and each additional pair of such interactions increases the relative energy. The highest energy isomer has all the nitrogens on the same face; this C_4 isomer is 3.35 kcal mol^{-1} above the S_8 conformer.

The conformation preference for the *s-trans* arrangement in the **3** and **4** nanohoops is even more pronounced that in **2**. The *s-cis* arrangement in **9b** and **10b** force the nitrogen lone pairs on adjacent rings to come together, leading to large destabilization. Introducing just two *s-cis* arrangements in [8]-**3** or [8]-**4** (Figures S3 and S4) leads to conformations that are 11 and 15 kcal mol^{-1}, respectively, above the all-*s-trans* structure. Therefore, hereafter we consider only the all *s-trans* conformation for **2**−**4**. Note that due to the symmetry of the

(21) Vaschetto, M. E.; Retamal, B. A.; Monkman, A. P.; Springborg, M. *J. Phys. Chem. A* **1999**, *103*, 11096–11103.
(22) Barone, V.; Minichino, C.; Fliszar, S.; Russo, N. *Can. J. Chem.* **1988**, *66*, 1313–1317.

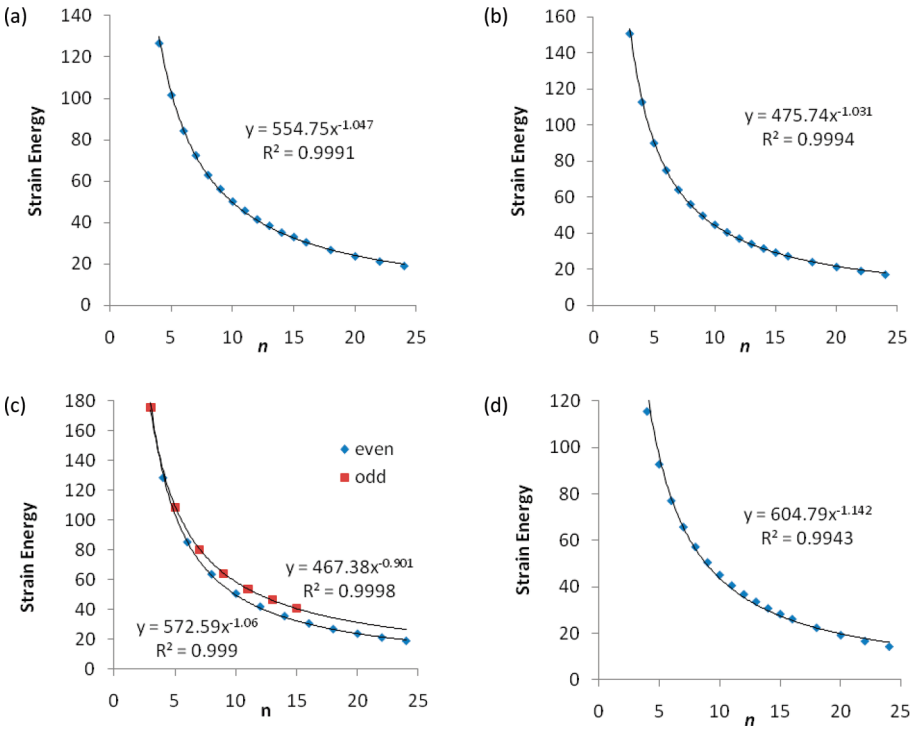

FIGURE 7. Correlation of strain energy (kcal mol^{-1}) with ring size for (a) **2**, (b) **3**, (c) **4**, and (d) **5**.

pyrimidinyl building block, this additional conformational complexity does not arise in **5**.

Strain energies of the **2**−**5** nanohoops are computed using reactions 2−5, which are analogues of reaction 1. The reference compounds used in these reactions are the ground-state conformations involving the all-*s*-*trans* arrangements. The B3LYP/6-31G(d)-computed strain energies are listed in Table 2.

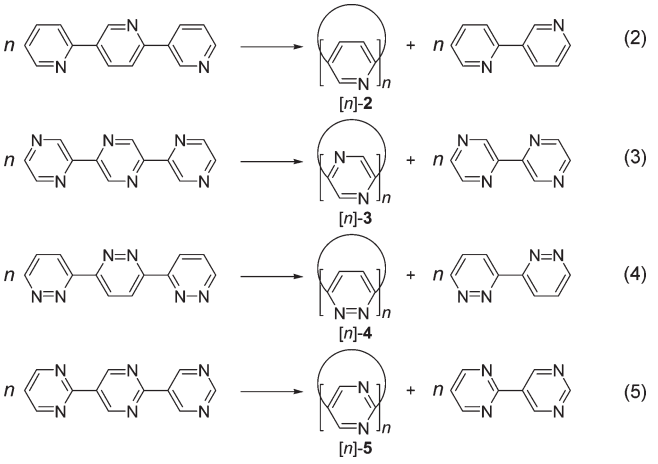

As for the paracyclophanes **1**, the strain energy of these nitrogen analogues decreases exponentially with increasing size of the hoop. These relationships are displayed in Figure 7. While there is some variation in the strain energies for the even- and odd-numbered nitrogen nanohoops as found for **1** (see Figure 2), the variation is small for **2**, **3**, and **5**. A single power series describes these sets of compounds very well. On the other hand, the variation between the even and odd number of repeat units in **4** is substantial (see Figure 7c). The odd members of **4** are substantially more strained than the even members.

The origin of the larger SE with the odd members of **4** lies in the preference for the *s*-*trans* arrangement of the nitrogens. For the even members of **4**, the diazo groups alternate from one side of the hoop to the other. However, with the odd members of **4**, there must be at least one *s*-*cis* arrangement of the diazo groups. The difference in SE predicted by the power functions fit for the even and odd series for [14]-**4**, [15]-**4**, and [16]-**4** is just over 8 kcal mol^{-1}, consistent with the difference in energy between the two conformers **10a** and **10b**. The dihedral angle between the two pyridzinyl rings with *s*-*cis* diazo groups is quite large, 20° in [11]-**4**, 24° in [13]-**4**, and 26° in [15]-**4**. This large twist is expected to minimize the interactions between the adjacent nitrogen atoms.

While there are *s*-*cis* and *s*-*trans* relationships possible in **3**, one can actually construct these nanohoops with either an even or odd number of pyrazinyl rings using only *s*-*trans* relationships. The odd members of **2** must have at least one *s*-*cis* relationship, but the energetic penalty for this relationship is expected to be very small, less than 1 kcal mol^{-1} based on the energy difference of **8a** and **8b**. There is no *cis*/*trans* relationship with **5**. Thus, we expect only **4** to display a large even/odd separation.

The different SE curves for the even and odd members of **1** result from the required, less energetically favorable, helical orientation of the phenyl rings within the odd series. Since one or two *o*,*o*′ interactions have been deleted in the nitrogen nanohoops relative to **1**, the preference for the alternating canting of the rings over the helical structure is reduced. The alternating ring structure in **2** is observed, but it differs from **1** in two important ways. First, the dihedral angles between the rings are smaller in **2** than **1**, generally being less than 15°. Second, a local helical arrangement has such a small

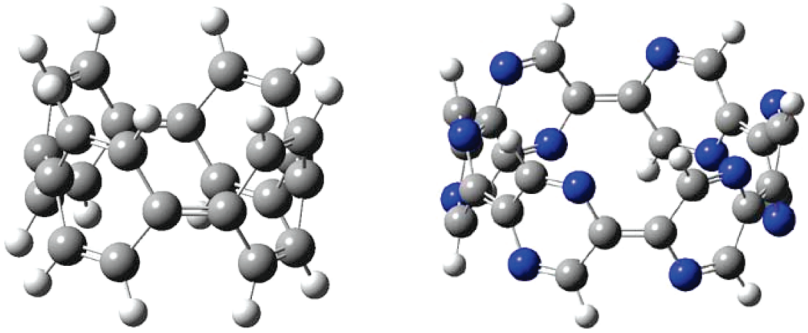

FIGURE 8. B3LYP/6-31G(d)-optimized structures of two representative examples of bond-shift isomers.

energetic affect that a single curve can be used to describe the SE of the even and odd members. For both **3** and **5**, the dihedral angles between the rings are quite small. For **3**, the dihedral angle is less than a degree for all members of the series, and for **5** the members with n greater than 8 all have dihedral angles less that 2°, with a decreasing value as n increases. Thus, there is essentially little even/odd variation for **2**, **3**, and **5**.

With Figure 4 we established that the strain energy of **1** largely reflects the energetic consequence of bending at C_1 and C_4 of each phenyl ring (along with the distortions at the *ortho* carbons). The same is true for the nitrogen-substituted nanohoops **2**−**5**. Linear relationships between the analogous bend angle and their strain energies are found for all four series and are displayed in Figure S6. Because of the strong n-even/odd strain dependence in **4**, we fit two lines in this case, one for the even members and one for the odd members. For all of the nanohoops examined here, the strain energy is largely predicted solely by the internal bend angle.

It is interesting to note that the bend angles of all five nanohoops **1**−**5** are quite similar for a given n value, varying by less than a degree. Furthermore, the value of the bend angle for a nanohoop with n rings is close to the value of the internal angle in a perfect polygon with $2n$ sides. While this *must* be true of a nanohoop of D_{nh} or C_{nh} symmetry, most of the nanohoops are not of these symmetries. This angle similarity suggests that the difference in the strain energies of the different nanohoops simply reflects the difficulty in bending the *para* hydrogen symmetrically out-of-plane of the different aromatic rings. To assess this, we computed the energies of the five building blocks of the nanohoops **1**−**5** with their *para* hydrogens bent out of the plane by varying angles, from in-plane to 20° out-of-plane. These bending curves are shown in Figure S7. Each of these bending energy curves can be nicely fit with a quadratic function, whose second derivative provides an estimate of the bending force constant. The bending forces increase in the order pyrazine < pyridazine < pyrimidine < pyridine < benzene.

If the strain energy of the nanohoops originates predominantly from the bend angle, as indicated for **1** (see Figure 3), then the strain energies of the nanohoops should be in the relative order **3** < **4** < **5** < **2** < **1**. Inspection of Tables 1 and 2 indicates that some of these trends do hold up. Nanohoops **1** are the most strained for all n except 13 and 15, where [13]-**4** and [15]-**4** are more strained due to the repulsions between adjacent nitrogen lone pairs. The small members of **3**, namely, $n \leq 10$, are the least strained nanohoops, and the larger nanohoops **3** are the second least strained among the set. The members of **5** are all less strained than the same-sized members of **1** and **2**.

But why are the nanohoops **5** the least strained of the larger nanohoops (and only slightly more strained than the smaller members of **3**)? Bend strain alone does not fully account for this; they should be more strained than either **3** or **4**.

Substitution of the C−H group with nitrogen allows for the possibility of weak electrostatic stabilization between rings, via the attraction of the nitrogen lone pair and the o'-hydrogen. The disubstituted nanohoops **3**−**5** have little canting between adjacent rings, affording approximately equidistant N···H separations. For example, the N···H distances in [16]-**3**, [16]-**4**, and [16]-**5**, are 2.543, 2.494, and 2.534 Å, respectively. Therefore, this interaction should be equally stabilizing of all three systems.

What does vary between **3**−**5** is the orientation of the dipole moment of each component ring. Pyrazine has no dipole moment, and so the interactions between the rings of **3** are negligible. The dipole moment of pyridazine is large (4.1 D), but within **4** the dipoles are arranged largely antiparallel, and so one might expect a small destabilizing interaction between rings. Pyrimidine has a moderate dipole moment (2.3 D) and the dipole moments align within **5**, offering an electrostatic stabilization of this class of nanohoop.

3.4. Alternate Structures: Bond-Shift Isomers and Möbius Conformations. In the search for conformers of [3]-**1** and [4]-**1**, we discovered an alternate isomeric form, a bond-shift isomer where instead of aromatic rings connected by single bonds, 1,4-cyclohexadienyl rings are connected by double bonds, such as [3]-**1bs** and [4]-**1bs**. The repeat unit is **11**. Examples of the structures of these bond-shift isomers are drawn in Figure 8. The energies of all located bond-shift isomers of the five types of nanohoops, relative to their aromatic analogues, are listed in Table 3.

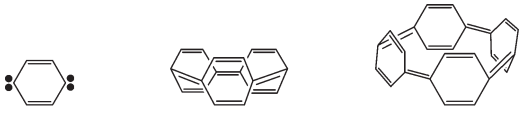

Given the energetic stability associated with aromatic rings, it is somewhat surprising that there are any bond-shift isomers at all. In fact, there are no bond-shift isomers for any nanohoops containing seven or more rings; only the canonical aromatic structures are located. For nanohoops **1**, **3**,

TABLE 3. Energies (kcal mol^{-1}) of Bond-Shift Isomers Relative to Their Aromatic Analogues

	E_{rel}		E_{rel}		E_{rel}
[3]-**1bs**	−34.59	[3]-**2bs**	[a]	[3]-**3bs**	−21.58
[3]-**1TS**	2.14			[3]-**3TS**	4.21
[4]-**1bs**	8.56	[4]-**2bs**	8.60	[4]-**3bs**	9.90
[4]-**1TS**	17.44	[4]-**2TS**	8.62	[4]-**3TS**	27.88
[5]-**1bs**	35.05			[5]-**3bs**	31.12
[6]-**1bs**	56.12			[6]-**3bs**	49.91
[3]-**4bs**	−27.75	[3]-**5bs**	[a]		
[3]-**4TS**	2.78				
[4]-**4bs**	18.02				
[4]-**4TS**	22.09				
[5]-**4bs**	43.60				
[6]-**4bs**	66.65				

[a]The corresponding aromatic structure could not be located.

TABLE 4. Aromatic Stabilization Energy (ASE, kcal mol^{-1}) and Delocalization Energy (DE, kcal mol^{-1}) of Nanohoop Building Blocks

compound	ASE	compound	DE
benzene	−33.9	**12**	−13.1
pyridine	−29.6	**13**	−11.4
pyrazine	−24.9	**14**	−8.7
pyridazine	−25.8	**15**	−13.0
pyrimidine	−24.5	**16**	−13.1

and **4**, bond-shift isomers were located and identified as local energy minima when the hoop contains three to six rings. For **2**, bond-shift isomers were located only for the hoops with three or four rings, and the only bond-shift isomer of **5** we located had three pyrimidinyl rings.

The structures of the bond-shift nanohoops display decided bond alternation. Within the rings, the six bonds differentiate into two short ones and four long ones. The C−C bonds between the rings are short, ranging from 1.36 Å in the nanohoops with three rings to 1.37 Å with four rings to 1.39 Å with five rings and 1.40 Å for the largest examples, which have six rings. The C−C distance in the aromatic nanohoops with ring count less than seven is typically about 1.49−1.54 Å.

Since the bond-shift isomers appear only with a small number of rings, it suggests that these alternate structures become feasible only when the aromatic structures are quite strained. The competition between the aromatic and bond-shift isomers is therefore a trade-off between the stability of the aromatic ring versus the delocalization of the highly conjugated bond-shift structure and the bend strain in the aromatic system versus the bend strain in the bond-shift system.

The aromatic stabilization energy (ASE) can be assessed using the method proposed by Schleyer,[23] an extension of the homodesmotic[24] and group equivalent[18] approaches. The reactions used to evaluate the ASE of the building blocks of **1**−**5** are shown in Scheme S1, and the ASE values, where the energies of all compounds were computed at B3LYP/6-31G(d), are listed in Table 4. Similarly, one can evaluate the delocalization energy (DE) of the building blocks of the bond-shift isomers, where the formal carbene centers are connected to a methylene group, as in **12**−**16**. The reactions utilized to evaluate their DEs are shown in Scheme S1, with the values included in Table 4.

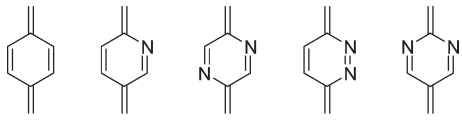

12 **13** **14** **15** **16**

The ability to bend at the *para* carbons of **12**−**16** was evaluated in a similar fashion to how we evaluated the bending in the aromatic species. The bend curves are shown in Figure S8. These curves are fit to a quadratic function. The estimated force constants increase in the order **14** < **15** < **13** < **16** < **12**. Most importantly, the force constants for bending in these bond-shift rings are about 50% that of the corresponding aromatic rings.

Bending at the *para* positions of the aromatic ring building blocks must lead to loss of ASE as the π overlap is diminished. The two rings with the stiffest bending force constant are the two with the largest ASE: benzene and pyridine. This succinctly explains why nanohoops **1** and **2** are the most strained for a given n value: bending is difficult and leads to loss of substantial ASE. That the members of **5** are generally the least strained reflects in part the fact that pyrimidine possesses the least ASE.

It also explains why the bond-shift isomers are observed for the smaller nanohoops. With these small hoops ($n \leq 6$), the bending is so severe that substantial strain and loss of ASE must be incurred by the aromatic structure. The alternative bond-shift structure, with a softer bending constant, can better accommodate severe bend angles. Further, the DE is relatively small, so its loss upon bending is less consequential.

In fact, for all five nanohoops composed of three rings, the bond-shift isomer is actually lower in energy than the aromatic structure. The extreme out-of-plane bending in these small nanohoops diminishes the ASE to such an extent that the bond-shift structure is preferred. In fact, we could not locate a stable structure for [3]-**2** or [3]-**5**; for these cases only the bond-shift isomer, [3]-**2bs** and [3]-**5bs**, could be located.

The canonical aromatic and bond-shift isomers are separated by a transition state, and we located these TSs for the nanohoops with three and four rings. The energies of these TSs are listed in Table 3, with the suffix "**TS**" added to the structure identifier. For **1**, **3**, and **4**, with three rings, where the bond-shift isomers are highly preferred over the aromatic form, the barrier from the aromatic isomer is very small, less than 5 kcal mol^{-1}. For the nanohoops with four rings, the barriers leading to the less stable bond-shift isomer are quite substantial, greater than 17 kcal mol^{-1}, except for the pyridine case, where the TS and bond-shift isomer are nearly isoenergetic.

While these bond-shift isomers are local energy mimima, they are unlikely to be prepared. The large bond-shift nanohoops are significantly higher in energy than their aromatic analogues, with large barriers for the conversion of the aromatic to bond shift form, and so the larger bond-shift isomers will be difficult to trap. The nanohoops with three rings are simply extraordinarily strained and therefore extremely difficult to prepare.

(23) Schleyer, P. v. R.; Puhlhofer, F. *Org. Lett.* **2002**, *4*, 2873–2876.
(24) Wheeler, S. E.; Houk, K. N.; Schleyer, P. v. R.; Allen, W. D. *J. Am. Chem. Soc.* **2009**, *131*, 2547–2560.

This last assertion was questioned by a referee, who noted that a substituted analogue of [2]-**1bs**, **17**,[25] has been prepared. Surely, if this even more highly strained species could be formed—we estimate the strain energy of [2]-**1bs** is 176 kcal mol^{-1} at B3LYP/6-31G(d)—then the nanohoops with three or four rings should be reasonable synthetic targets. However, **17** is really quite different than [2]-**1bs**. The four appending phenyl groups effectively diminish the bond order of the formal double bonds of the cyclophenylene. This will radically reduce its strain. Using reaction 6, we estimate the strain energy of **17** is 94 kcal mol^{-1}, about half that of [2]-**1bs**! Furthermore, the strain energy of the analogous phenylated [3]-**1bs**, **18**, has a strain energy of 59.8 kcal mol^{-1} (reaction 7), almost 100 kcal mol^{-1} less than the strain of [3]-**1bs**. The fact that **17** can be prepared really tells us nothing about the potential existence (or lack thereof) of [2]-**1bs** or other small nanohoops. The only other report of a preparation of [2]-**1bs** contends that a dicyano version was potentially formed, as evidenced by trapped products.[26] However, the cyclophane itself was not directly identified nor isolated. We therefore believe that the very small *unsubstituted, parent* nanohoops will be very difficult to prepare and isolate.

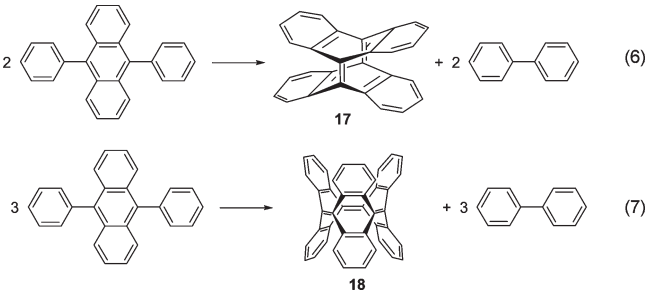

Bertozzi[2] mentioned locating Möbius-strip arrangements of [9]-**1**, [10]-**1**, and [12]-**1**, where successive rings are canted in the same helical direction by about 35°. These were all at least 2 kcal mol^{-1} per ring higher in energy than the lowest energy conformer. Dihedral angles of this value would actually produce nanohoops with about one full twist, not the half-twist of a Möbius strip. The dihedral value for a Möbius-strip nanohoop should be about 180°/n, or about 20° for nanohoops of the type Betozzi examined. This ideal Möbius dihedral value is far from the typical dihedral value in the normal conformers of **1** or any of the other nanohoops for that matter. This suggests that a Möbius-strip arrangement would be inherently strained relative to the alternating ring structures. Nevertheless, a Möbius-strip arrangement for the odd-n nanohoops **2** and especially **4** would potentially eliminate the one very close interaction of the nitrogens. This conformation would have *s-trans*-like arrangements of the nitrogens of adjacent rings all the way around the nanohoops.

The above discussion presumes that the Möbius-strip nanohoops would have small writhe, allowing for other values of the dihedral twist.[27] The Möbius polyporphirins have large writhe.[28−32] Rzepa has demonstrated a number of Möbius structures with substantial writhe.[31,33−35] The polythiocyanogens, especially with 16 repeat units,[34] and the polyporphyrins might suggest that the nanohoops discussed here might also display large writhe. However, the nanohoops described here require that the repeat units be attached in a *para* relationship. This makes it very difficult to create the sharp turns needed to create a "figure 8" structure or the complicated twisting seen in the polyporphirins and polythiocyanogens. These polymers are built from building blocks that allow connections of angles far less than 180°, something that the paracyclophanes and related compounds simply cannot adopt. It does suggest that the metacyclophanes might adopt Möbius structures analogous to the polyporphirins and polythiocyanogens.

Nonetheless, we searched for Möbius-strip nanohoops with varying number of rings and for the different building blocks. The Möbius strips should have C_2 symmetry. However, in all cases optimizations of a Möbius-strip arrangement that began with a structure with appropriate dihedral angles between the rings invariably collapsed to structures that had only local helical arrangements and with large stretches of alternating back-and-forth rings. (Figure S9 shows an example of an initial Möbius-strip arrangement of [9]-**1** and its final optimized arrangement.) In other words, we were unable to locate any true Möbius-strip arrangement of any nanohoop, regardless of size or building block type.

3.5. Ribbon Nanohoop Structures. Our ultimate goal was to suggest nanohoops that have ribbon-like structure. The best examples of this ideal are the members of **5**. These nanohoops have a small dihedral angle between the rings: for the larger hoop this dihedral angle is less than 2°. In addition, these nanohoops are of C_{nh} symmetry. This means that the top and bottom halves of the hoop are mirror-images, suggesting a real ribbon structure. Examples of these are shown in Figure 9.

A measure of the resiliency of the ribbon structure is the energy needed to rotate a ring out of the ribbon. We have computed the transition state for the rotation of one ring in [8]-**5**, [10]-**5**, [12]-**5**, and [14]-**5**. The structure of the rotational TS [10]-**5ts** is shown in Figure 9. The computed rotational barriers are 21.77, 19.21, 17.96, and 17.22 kcal mol^{-1} for the 8-, 10-, 12-, and 14-ring systems, respectively. The rotational TSs are of C_s symmetry, and so the rotated pyrimidinyl ring and all of the *para* carbons must lie in the same plane. These atoms must form the closed cycle, and as the hoop gets smaller, strain is built up, especially at the *para* carbons of the in-plane ring as significant angle distortions are required to keep the ring closed.

For comparison, the rotational barrier for flipping a phenyl ring in [10]-**1** and [12]-**1** is 9.4 and 7.8 kcal mol^{-1}, respectively, about 10 kcal mol^{-1} smaller than the rotational

(25) Viavattene, R. L.; Greene, F. D.; Cheung, L. D.; Majeste, R.; Trefonas, L. M. *J. Am. Chem. Soc.* **1974**, *96*, 4342–4343.
(26) Tsuji, T.; Okuyama, M. *Chem. Commun.* **1997**, 2151–2152.
(27) Fowler, P. W.; Rzepa, H. S. *Phys. Chem. Chem. Phys.* **2006**, *8*, 1775–1777.
(28) Shimizu, S.; Aratani, N.; Osuka, A. *Chem.—Eur. J.* **2006**, *12*, 4909–4918.
(29) Rzepa, H. S. *Org. Lett.* **2008**, *10*, 949–952.
(30) Tanaka, Y.; Saito, S.; Mori, S.; Aratani, N.; Shinokubo, H.; Shibata, N.; Higuchi, Y.; Yoon, Z. S.; Kim, K. S.; Noh, S. B.; Park, J. K.; Kim, D.; Osuka, A. *Angew. Chem., Int. Ed.* **2008**, *47*, 681–684.
(31) Rzepa, H. S. *Org. Lett.* **2009**, *11*, 3088–3091.
(32) Tokuji, S.; Shin, J.-Y.; Kim, K. S.; Lim, J. M.; Youfu, K.; Saito, S.; Kim, D.; Osuka, A. *J. Am. Chem. Soc.* **2009**, *131*, 7240–7241.
(33) Allan, C. S. M.; Rzepa, H. S. *J. Org. Chem.* **2008**, *73*, 6615–6622.
(34) Allan, C. S. M.; Rzepa, H. S. *Dalton Trans.* **2008**, 6925–6932.
(35) Wannere, C. S.; Rzepa, H. S.; Rinderspacher, B. C.; Paul, A.; Allan, C. S. M.; Schaefer Iii, H. F.; Schleyer, P. v. R. *J. Phys. Chem. A* **2009**, *113*, 11619–11629.

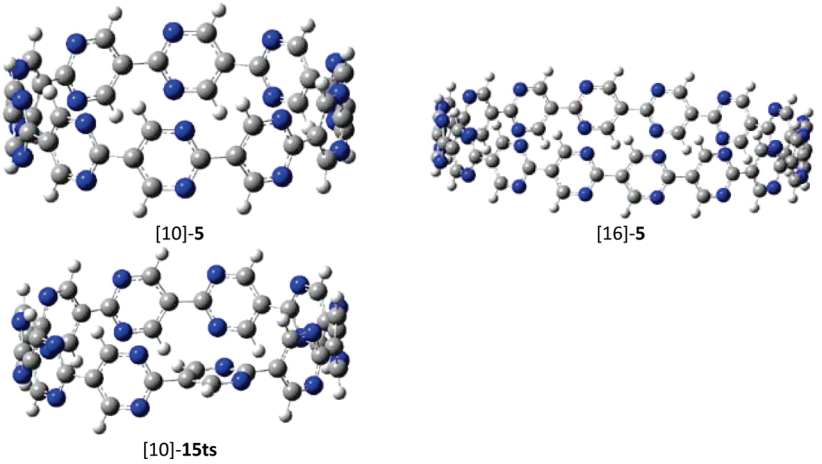

FIGURE 9. B3LYP/6-31G*-optimized structures of [10]-**5** and [16]-**5** and the transition state for rotation of one pyrimidine group ([10]-**5ts**).

barriers in [10]-**5** and [12]-**5**. The pyrimidine nanohoops are therefore much more rigid and resistant to deformations than the cycloparaphenylenes.

4. Conclusion

The nanohoop is an interesting chemical structure that has only recently been explored. The paracyclophanes **1** were found to be fairly strained, even when the hoop contains 20 phenyl groups.[6] Increasing the size to 24 phenyl groups reduces the total strain energy to 24 kcal mol^{-1}, or about 1 kcal mol^{-1} per phenyl group. Relatively strain-free nanohoops will, therefore, require very large *n* values.

The phenyl rings of the paracyclophanes **1** preferably cant in alternating directions. The odd members of **1** have one helical section, where three consecutive phenyls twist in the same direction, making the odd members slightly more strained than the even members. To diminish this ring canting, caused by *o*,*o*′-interactions, we examined the nanohoops where one or two *ortho* C−H groups are replaced by nitrogen. This eliminates the steric repulsion and leads to nanohoops with much less alternation of the rings. In fact, nanohoops **3** and **5** have dihedral values between adjacent rings of less than 2°.

The strain energies of the different nanohoops correlate very closely with the bend angle, defined as $C_{1'}-C_1-C_4$. In fact for a given *n* value (the number of rings within the nanohoop) the different nanohoops **1**−**5** have very similar bend angles. The fact that the nanohoops exhibit different strain energies, with **3** and **5** being the least strained and **1** and **2** the most strained, suggests that the aromatic building blocks respond differently to bending at the *para* positions. The aromatic building blocks with the most aromatic stabilization energy, benzene and pyridine, have the stiffest bending force constants. These aromatic rings are resistant to the bending that is needed to form the hoops and result in large SE of their respective nanohoops. Pyrimidine has a smaller bending force constant. Coupled with the weak electrostatic interactions between neighboring nitrogen lone pairs and *ortho* hydrogens and the alignment of the dipole moment of the pyrimidinyl rings, the members of **5** are the least strained nanohoops.

A bond-shift isomer is found for the smallest nanohoops ($n \leq 6$). These isomers replace the aromatic ring with a 1,4-cyclohexadienyl or analogous nitrogen-substituted system connected by double bonds. The loss of aromaticity in forming these conjugated isomers is made up for by substantially weaker force constants associated with the out-of-plane bending. In fact, for the very strained nanohoops with three rings, the bond-shift isomer is lower in energy than the aromatic analogue. Nonetheless, these bond-shift isomers are quite strained and are unlikely to be observed.

In the search for potential novel nanohoops, we suggest that efforts be made toward the synthesis and characterization of the nitrogen-substituted analogues described here, but especially the nanohoops **5**. These nanohoops are generally less strained than the others, making them potentially easier to construct. Their high-symmetry minimum energy geometry gives them a ribbon-like structure. The ribbon is fairly robust, with large barriers for rotation of a pyrimidinyl ring, much larger than for phenyl rotation in the cycloparaphenylenes. The nanohoop ribbons **5** might possess interesting properties. They may be novel guests with tunable diameter, although the other nanohoops are likely to also be fine hosts, as an induced-fit ribbon-like structure is probable. They might stack in the solid state, creating tunnels and passages. We look forward to their synthesis and characterization.

Acknowledgment. This work was supported by The Welch Foundation (W-0031) and Trinity University.

Supporting Information Available: Full citation of ref 11, Figures S1−S8, Tables S1−S3, Scheme S1, and optimized coordinates at B3LYP/6-31G(d) and M06-2x/6-31G(d) for **1**−**5**. This material is available free of charge via the Internet at http://pubs.acs.org.